https://doi.org/10.48048/tis.2023.5675

Schiff Bases Ligands Derived from *o*-Phthalaldehyde and Their Metal Complexes with Cu^{2+} and Ni^{2+}: Synthesis, Anti-Breast Cancer and Molecular Docking Study

Adnan Taleb Nasser[1,2] and Rafid Humaidan Al-Asadi[1,*]

[1]Department of Chemistry, College of Education for Pure Sciences, University of Basra, Basra 61004, Iraq
[2]Hamdan Girls High School, Education Directorate of Basrah, Ministry of Education, Basrah 61004, Iraq

([*]Corresponding author's e-mail: dr.rafid74@yahoo.com)

Received: 19 August 2022, Revised: 15 October 2022, Accepted: 22 October 2022, Published: 31 May 2023

Abstract

The Schiff bases and their complexes have an observed biological efficacy, so in the current study it has been prepared, characterized and evaluated the biological activity of some Schiff bases and their metal complexes with copper and nickel and based on ortho-phathaldehyde as a primary compound. A new Schiff bases ligands and metal complexes $\{[Cu(L)_n(H_2O)_2]Cl_2.mH_2O$ and $[Ni(L)_n].mH_2O$, where L=N',N'''-((1E,1'E)-1,2-phenylenebis(methanylylidene)) di(benzohydrazide) L^1, N',N'''-((1E,1'E)-1,2-phenylenebis (methanylylidene)) di(isonicotinohydrazide) L^2, 1,2-bis((E)-(2-(2,4,6-trichlorophenyl)hydrazono)methyl) benzene L^3 ; n = 1, 2 ; m = 0, 1, 3/2, 5/2$\}$ have been synthesized and elucidated by mass, FT-IR, ^{13}C and $^{1}HNMR$, molar conductivity, flame-atomic absorption, magnetic susceptibility, Powder-XRD and TG analysis. The results showed that the L^1 and L^2 ligands behave as a tetra-dentate donor and were associated with metal ions in a molar ratio of 1:1, while L^3 ligand was bi-dentate donor and associated with metal ions in 1:2 molar ratio. In addition, the geometric shapes of the prepared complexes were tetrahedral and square planar for Ni^{2+} and Zn^{2+} complexes, and octahedral for Cu^{2+} complexes. The effect of cellular toxicity in the laboratory has been examined by MTT assay for all compounds against the MCF-7 cancer breast cell line and found to have low efficacy except $[Cu(L^3)_2(H_2O)_2]$ $Cl_2.H_2O$ (5). The copper complex's molecular docking has been performed with breast cancer proteins using the MOE program, and found to target ERα, CDK6 and EGFR proteins by binding to hydrogen bonds and *pi*-interactions.

Keywords: Schiff base, Metal complexes, Molecular docking, Breast cancer, *o*-Phthalaldehyde, MTT, Breast cancer, MOE program

Introduction

Over a long time, Schiff bases take off consideration since of their application in science, such as; antibacterial, anticorrosion, antifungal, anticancer, antioxidant, and their extraordinary affectability, selectivity, and steadiness toward some metal ions [1-5].

Schiff's bases have an imperative part to play within the improvement of coordination and therapeutic chemistry since they effectively frame for metal complexes molecules [6]. These compounds are played within the field of bioinorganic chemistry and different angles of organo-metallic compounds [7,8]. In addition, they were utilized as electronic sources and photonic and laser components because they possessed non-linear visual properties [9,10].

Schiff bases and their complexes containing the azomethine group (-HC=N-). It is shaped by means of the condensation of the primary amines (RNH_2) and the carbonyl compound. The group (-HC=N-) is mainly appropriate for binding to metal ions through the lone pair of nitrogen atom [11].

Transitional metals complexes containing the Schiff base ligands that are linked through nitrogen and oxygen atoms have been of investigate significance over the past a long time and act as active locales and in this manner catalyze chemical reactions [12,13].

Ortho-phthalaldehyde has been applied as an extensively necessary source material in the synthesis and scientific research of Schiff bases, and it contains 2 carbonyl groups that have the ability to react with

nucleophilic reagents to produce di-azomethine compounds. Many research used *o*-phthalaldehyde as a source of the production of Schiff bases, which were later used as ligands to prepare many coordination metal-complexes [14-16].

Cancer is a category of diseases in which a group of cells leads to uncontrolled growth. The drugs that exist to treat cancer are not good enough, so developing more effective chemotherapy drugs is the main challenge for researchers over the years. Breast cancer is the most common malignant tumor in women worldwide and can be treated in ~70 - 80 % of patients with non-metastatic disease in its early stages. Several studies have shown the susceptibility of Schiff base compounds and their metallic complexes to inhibit breast cancer cells [17,18].

The current study focuses on synthesis and identification of some Schiff bases compounds which contains di-azomethine group and their coordination complexes with Copper (II) and Nickel (II) and the study of their effect as anti-breast cancer as well as the study of molecular docking of molecules that have shown effectiveness to find out where to interact with cancer cell proteins.

Materials and methods

The chemicals used in the current study were obtained from well-known companies and used without purification after confirming their melting points. Infrared spectra recorded using Shimadzu model IR Affinity-1 device, using KBr discs between 4,000 - 400 cm^{-1}. The ^{1}H and ^{13}C NMR spectra were recorded using Bruker 500 MHz spectrometer with DMSO-*d6* acting as a solvent. EI technique used to record compounds mass spectra with Agilent Technologies 70 eV spectrometer. TG and DTG measurements under nitrogen were made within a range 25 - 750 °C using the SDT Q600 V20.9 Build 20. The magnetic susceptibility of metal complexes was measured by a Sherwood-scientific magnetic balance at room temperature and using powder samples. Molar conductance of metal-complexes was measured at room temperature in DMSO solvent using HI 2315 Conductivity Meter, and with a concentration (1×10^{-3} M). The percentage of Cu(II) and Ni(II) ions was estimated using the flame atomic absorption technique, and using Sense AA GBC Scientific Equipment device. Powder XRD patterns recorded by Philips X pertpro MPD diffractometer with using Cu K as source, λ=1.5406 Å and Ni as a filter.

Synthesis of ligands

N', N'"-((1E,1'E)-1,2-phenylenebis(methanylylidene)) di(benzohydrazide) L^1

Solution (10 mmol) 1.36 g of benzohydrazide in 10 mL EtOH absolute gradually added to a solution (10 mmol) 1.34 g of o-phthalaldehyde in 10 mL EtOH absolute with a few drops of glacial HAc. The mixture was refluxed with stirrer for 2 h. and followed by TLC (ethyl acetate: chloroform, 4:1). The result was cold, filtered and re-crystallized with absolute ethanol. The product was yellow solid crystal. Yield: 84 %, mp: 170 - 172 °C. IR spectrum, ν, cm^{-1}: 3,414 and 3,261 (N–H), 3,064 (Ar–CH), 1,656 (C=O), 1,606 (C=C), 15,62(C=N). ^{1}H NMR spectrum, δ, ppm: 7.96 - 7.39 m (7H, Ar–H), 8.96 s (1H, CH=N), 12.05 s (1H, NH). ^{13}C NMR spectrum, δ_C, ppm: 120.34 (C_{8+10}), 123.04(C_1), 128.20(C_2), 130.37(C_9), 132.43(C_1), 133.30(C_2+C_9), 133.78(C_3+C_6), 146.75(C_4), 163.70(C_5). MS (EI, m/z (%)): 370[M^+, 0.8].

N', N'"-((1E,1'E)-1,2-phenylenebis(methanylylidene)) di(isonicotinohydrazide) L^2

A similar procedure is used as in L^1, but used (10 mmol) 1.37 g of isonicotinohydrazide instead of benzohydrazide. The product was a yellow-white crystal. Yield: 89 %, mp: 167 - 168 °C. IR spectrum, ν, cm^{-1}: 3,414 and 3,238 (N–H), 3,070 and 3,049 (Ar–CH), 1,662 (C=O), 1,616(C=C), 1,552(C=N). ^{1}H NMR spectrum, δ, ppm: 6.68 d (2H, Ar–H_b+$H_{b'}$), 6.79 d (1H, Ar–H_d), 7.49 - 7.20 m (3H, Ar–H), 7.93 s (1H, CH=N), 9.30 s (1H, NH). ^{13}C NMR spectrum, δ_C, ppm: 113.08(C_{7+10}), 119.86(C_1+C_2), 122.80(C_3), 129.25(C_8+C_9), 134.63(C_6), 148.53(C_4), 165.52(C_5). MS (EI, m/z (%)): 371[M^++1, 10].

1,2-bis((E)-(2-(2,4,6-trichlorophenyl) hydrazono) methyl) benzene L^3

A similar procedure is used as in L^1, but used (10 mmol) 2.11 g of (2,4,6-trichlorophenyl) hydrazine instead of benzohydrazide. The product was a yellow crystal. Yield: 82 %, mp: 179 - 180 °C. IR spectrum, ν, cm^{-1}: 3,321 (N–H), 3,078 (Ar–CH), 2,860 (Alph–CH), 1,590(C=C), 1,554(C=N). ^{1}H NMR spectrum, δ, ppm: 7.34 d (1H, H_c), 7.64 s (2H, Ar–H_b+$H_{b'}$), 7.76 d (Ar–1H, H_a), 8.46 s (1H, CH=N), 9.67 s (1H, NH). ^{13}C NMR spectrum, δ_C, ppm: 127.06(C_1), 127.57(C_{7+9}), 127.82(C_2), 128.85(C_3) 129.38(C_6+C_{10}), 132.85(C_8), 137.71(C_5), 138.63(C_4). MS (EI, *m/z* (%)): 521[M^+, 0.9].

Synthesis of metal complexes

General procedure

The hot methanolic solution of (1 mmol) of L^1 or L^2 or (2 mmol) of L^3 ligands were gradually added to (1 mmol) of hot methanolic solution of metal chloride (Metal = Cu(II) or Ni(II)) with stirring and

refluxing for 6 - 8 h. The precipitated products were filtered off, washed with water, methanol and diethyl ether. Then it dried and was obtained;

$[Cu(L^1)(H_2O)_2]Cl_2$ (1): Dark yellow colour. Yield: 76 %, mp: 249 °C dec. IR spectrum, ν, cm^{-1}: 3,477 (O–H), 3,414 (N–H), 3,070 and 3,045 (Ar–CH), 1,616(C=C), 1,573(C=N). Found, %: Cu 11.73. $C_{22}H_{24}Cl_2CuN_4O_4$. Calculated, %: Cu 11.69. μ_{eff} (B.M): 1.88. Molar conductivity (DMSO, $Ohm^{-1}cm^2mol^{-1}$): 73.3.

$[Ni(L^1)].H_2O$ (2): Red colour. Yield: 82 %, mp: > 300 °C. IR spectrum, ν, cm^{-1}: 3,444 (O–H), 3,387 (N–H), 3,062 (Ar–CH), 1,591(C=C), 1,554(C=N). Found, %: Ni 14.21. $C_{22}H_{22}N_4NiO_3$. Calculated, %: Ni 13.14. μ_{eff} (B.M): 2.84. Molar conductivity (DMSO, $Ohm^{-1}cm^2mol^{-1}$): 3.3.

$[Cu(L^2)(H_2O)_2]Cl_2$ (3): Green colour. Yield: 68 %, mp: > 300 °C. IR spectrum, ν, cm^{-1}: 3,514 (O–H), 3,446 and 3,363 (N–H), 3,086 and 3,057 (Ar–CH), 1,645 (C=C), 1,608 (C=N). Found, %: Cu 11.69. $C_{22}H_{22}Cl_2CuN_6O_4$. Calculated, %: Cu 11.67. μ_{eff} (B.M): 1.91. Molar conductivity (DMSO, $Ohm^{-1}cm^2mol^{-1}$): 63.7.

$[Ni(L^2)].5/2H_2O$ (4): Yellow colour. Yield: 80 %, mp: > 300 °C. IR spectrum, ν, cm^{-1}: 3,442 (O–H), 3,390 (N–H), 1,608(C=C), 1,566(C=N). Found, %: Ni 14.56. $C_{20}H_{23}N_6NiO_{4.5}$. Calculated, %: Ni 12.27. μ_{eff} (B.M): 3.10. Molar conductivity (DMSO, $Ohm^{-1}cm^2mol^{-1}$): 4.2.

$[Cu(L^3)_2(H_2O)_2]Cl_2.H_2O$ (5): Yellow colour. Yield: 59 %, mp: > 300 °C. IR spectrum, ν, cm^{-1}: 3,221 (O–H), 3,190 (N–H), 3,078 (Ar–CH), 2,880 (Alph–CH), 1,585(C=C), 1,539(C=N). Found, %: Cu 5.31. $C_{40}H_{30}Cl_{14}CuN_8O_3$. Calculated, %: Cu 5.16. μ_{eff} (B.M): 1.76. Molar conductivity (DMSO, $Ohm^{-1}cm^2mol^{-1}$): 76.1.

$[Ni(L^3)_2].3/2H_2O$ (6): White colour. Yield: 45 %, mp: 277 °C dec. IR spectrum, ν, cm^{-1}: 3415 (O–H), 3,323 and 3,302 (N–H), 3,078 and 3,047 (Ar–CH), 2,860 (Alph–CH), 1,581(C=C), 1,556(C=N). Found, %: Ni 4.91. $C_{40}H_{27}Cl_{12}N_8NiO_{1.5}$. Calculated, %: Ni 5.20. μ_{eff} (B.M): 0.89. Molar conductivity (DMSO, $Ohm^{-1}cm^2mol^{-1}$): 15.2.

Anti-cancer activity

MTT assay [19] was employed to test *in-vitro* cytotoxicity of studied compounds. Human breast cancer (MCF-7 cell line) was obtained from National Cell Bank of Iran. Cells grew in RPMI-1640 (Gibco) and DMEM medium (Gibco), respectively, with 10 % FBS (Gibco) supplemented with anti-biotic (100 U/mL penicillin and 100 µg/mL streptomycin). Cells were kept at 37 °C under wet air containing 5 % CO_2 and passed utilizing trypsin/EDTA (Gibco) and phosphate- buffered saline solution (PBS). The cultured media and conditions used for cell culture as 3D colonies were the same as single-layer cell culture.

Molecular docking

Molecular docking study of compound 5 was conducted using MOE (Molecular Operating Environment) 2019. The crystal structure of proteins was obtained from Protein Data Bank (PDB) (https://www.rcsb.org/ structure). Processing of study compound, proteins and docking procedures was carried out in accordance with literature [20].

Results and discussion

The condensation reaction between *o*-phthalaldehyde and some hydrazine derivatives at a 1:2 mole ratio gave Schiff bases ligands L^1, L^2 and L^3, **Figure 1** (i). Reaction of L^1 and L^2 ligands with Cu(II) and Ni(II) ions in methanol gave the complexes (1 - 4) by a 1:1 ratio, **Figure 1** (ii) a, while reaction of L^3 ligands with Cu(II) and Ni(II) ions gave the complexes (5,6) with 1:2 mole ratio, **Figure 1** (ii) b.

Characterization methods

The proposed structure of ligands was created by mass, infrared and nuclear magnetic resonance techniques. Mass spectra of prepared ligands showed molecular ion peak at *m/z* = 370, 371 and 521 for L^1, L^2 and L^3, respectively, but with low relative abundance, and the appearance of a set of fragments which indicating the presence of the proposed compound. The mass spectra of complexes did not exhibit the peaks that due to their molecular ions. However, it has shown the fragments confirming the presence of these compounds.

The FT-IR spectra for synthesis compounds showed weak bands at range 3,446 - 3,238 cm^{-1} which assign to stretching vibration of –NH groups, and 1 or 2 bands at the range between 3,045 - 3,086 cm^{-1} due to symmetrical and asymmetrical stretching vibration of C - H aromatic. In addition to, the strong band at range 1,608 - 1,552 cm^{-1} attributed to stretching vibration of azomethine group, this band has a shifting in complexes compounds due to the coordination between metals and ligands. The L^1 and L^2 compounds were characterized by the appearance of a strong band at 1,656 and 1,662 cm^{-1} due to the

presence of the carbonyl group, this band has disappeared in the coordination complexes, it is evidence the participation of C=O group in the coordinate process. The spectra of complexes were also characterized by the appearance of the stretching vibration of OH group as a broad band in the range 3,221 - 3,514 cm^{-1} because it contained the coordinate and lattice water molecules.

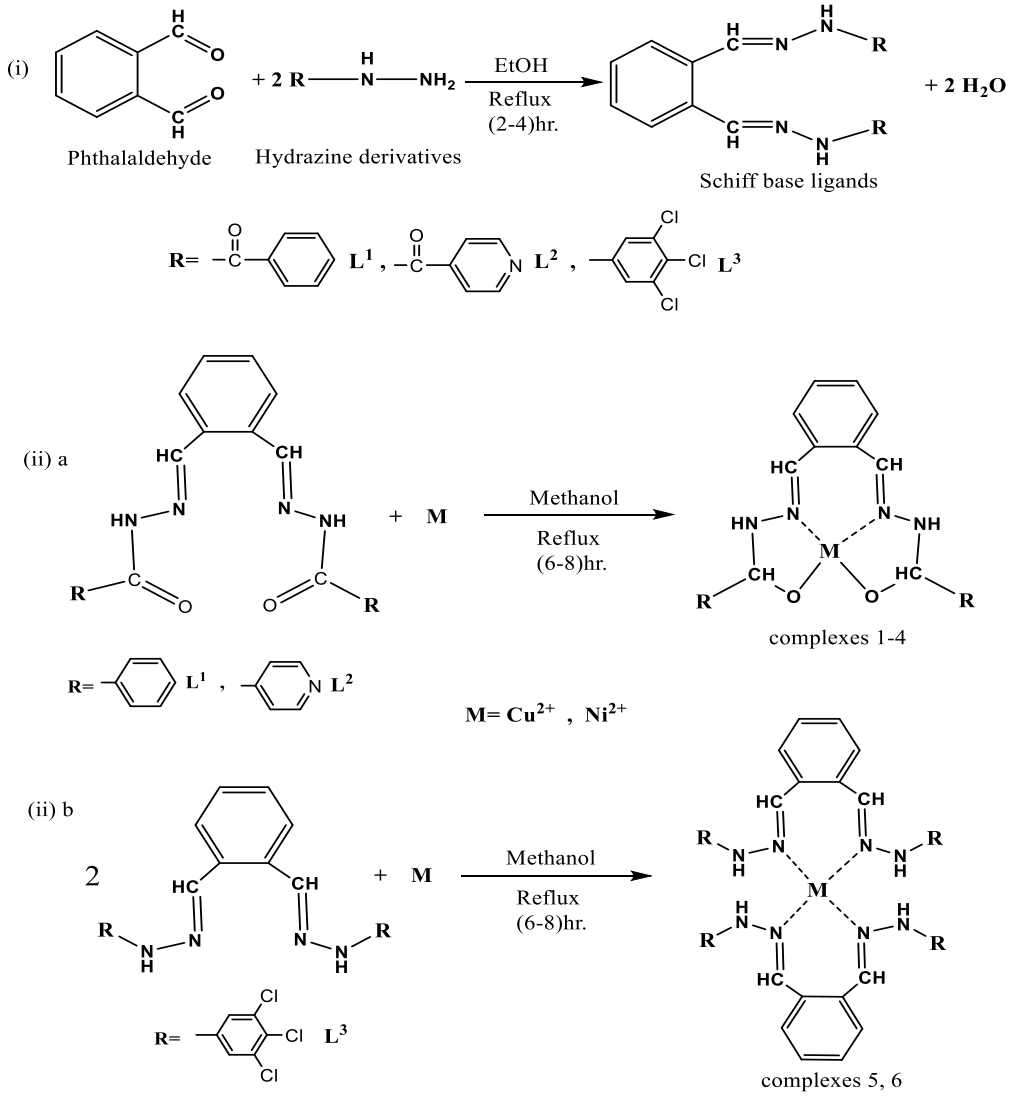

Figure1 Preparation pathway to ligands and metal complexes.

^{1}HNMR spectra of ligands, **Figure 2**, demonstrated a singlet, doublet and multiplet signals at the range 6.68 - 7.96 ppm that can be attributed to aromatic protons. The spectra confirmed the presence of the azomethine group with the appearance of a singlet signal at 8.96, 7.93 and 8.46 ppm for L^1, L^2 and L^3, respectively, while proton of amide group (−NH) appeared as a singlet signal at the 12.05, 9.30 and 9.67 ppm. ^{13}CNMR spectra have proven the correct skeletal structure of the prepared ligands. The signals at 163.70 ppm for L^1 and 165.52 ppm for L^2 assign to carbons of C=O group, while the signals at 146.75, 148.53 and 138.63 ppm for L^1, L^2 and L^3 were due to carbon of azomethine group. Aromatic carbons appeared in the range of 113.08 - 137.71ppm.

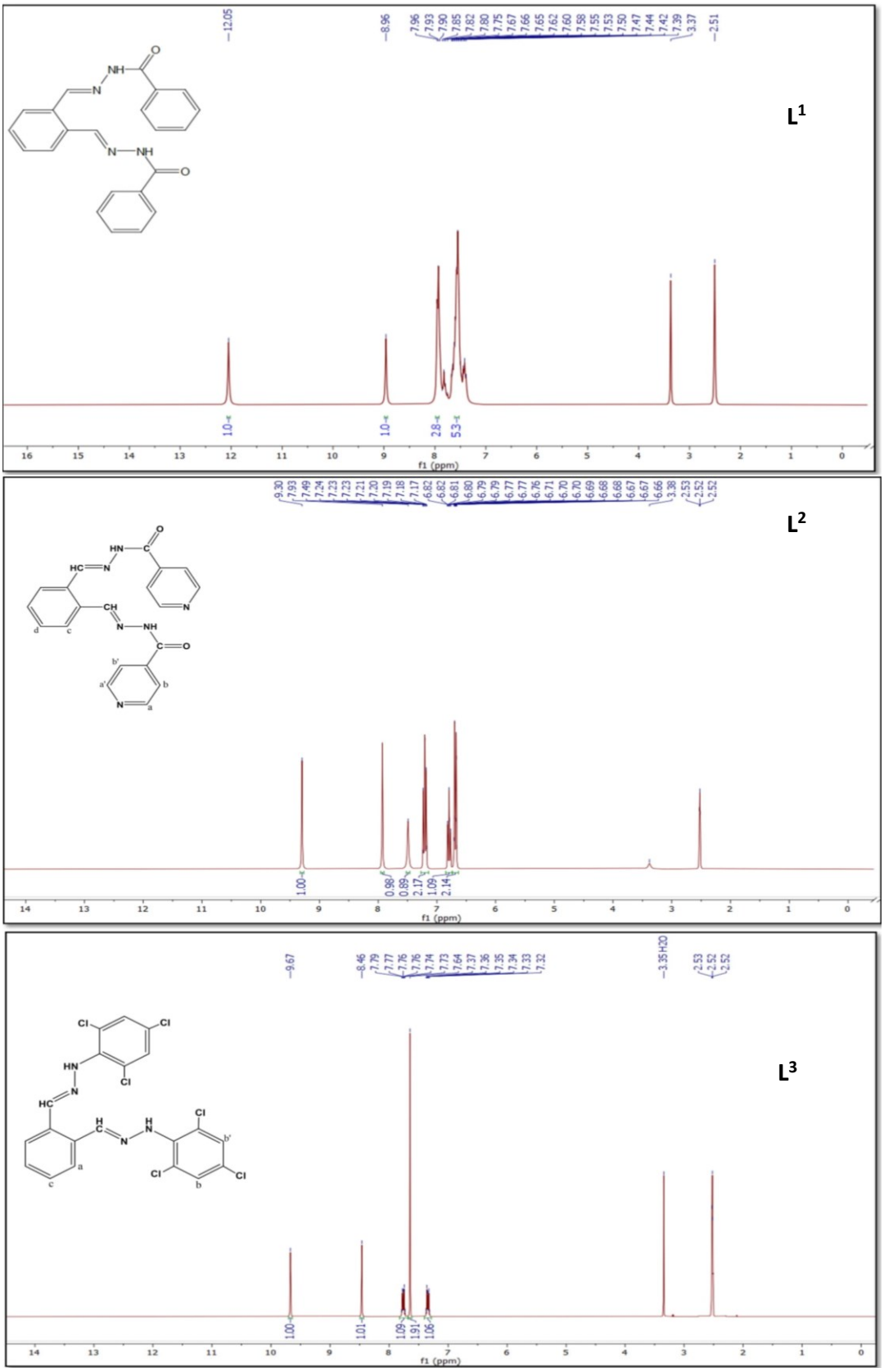

Figure 2 [1]HNMR spectra of ligands L^1, L^2 and L^3.

The metal: Ligand mole ratio of complexes determined by flame-atomic absorption, it was found that the Cu(II) and Ni(II) ions formed 1:1 chelates with L^1 and L^2 ligands, while was formed 1:2 chelates with L^3. The molar conductivity values of Cu-complexes were found to be located in the range of 63.7 - 76.1 Ohm^{-1} cm^2 mol^{-1}, where they are predicted to possess electrolyte properties and containing a counter-ion, while Ni- complexes were conductive values within range 3.3 - 15.2 Ohm^{-1} cm^2 mol^{-1}, which confirm that they did not contain counter ions with non-electrolyte properties [21].

The values of effective magnetic moment (μ_{eff}) of Cu- complexes, 1, 3 and 5, were at range 1.76 - 1.91 B.M, which indicates that they contain 1 unpaired electron in *d*-orbital and not found the participation of the orbitals magnetic moment, so the suggested geometric shape around copper ion in these complexes is octahedral (sp^3d^2). Ni-Complexes, 2 and 4, μ_{eff} value was (3.3 and 4.2 B.M), respectively, that this data indicates the presence of 2 unpaired electrons in *d*-orbital (high spin system), in addition to the presence of the orbitals moment contribution, so the expected geometric shape of these complexes is tetrahedral (sp^3), but complex 6, the value of μ_{eff} was 0.89 B.M, these value refers that it has diamagnetic (low spin system) and that its geometric shape is a square planar (dsp^2) [22].

Figure 3 and **Table 1** show the stages of thermal decomposition of metal complexes, the decomposition stages and thermograms refer the presence of lattice and coordinated water in structure of complexes molecules, which decompose in the early stages of disintegration at range 50 - 272 °C, while the other stages included the loss of parts of the ligands.

Table 1 Thermogravimetric analysis data of metal complexes.

Complexes	Stages	Temp. range (°C)	Decomposition parts	Weight loss %	
				Calculated	Found
$[Cu(L^1)(H_2O)_2]Cl_2$	1	50 - 272	$2H_2O$	6.65	6.37
	2	272 - 345	Cl_2	13.12	12.95
	3	345 - 394	CO_2	8.13	7.67
$[Ni(L^1)].H_2O$	1	50 - 145	H_2O	4.02	3.09
	2	145 - 293	NH	3.35	3.31
	3	293 - 362	C_7H_7N	23.48	23.93
	4	362 - 475	C_7H_7	20.35	20.03
$[Cu(L^2)(H_2O)_2]Cl_2$	1	50 - 242	$2H_2O+CO_2$	14.73	11.58
	2	242 - 292	CH_2N_2	8.28	7.91
	3	292 - 378	C_8H_6	20.11	20.47
$[Ni(L^2)].5/2H_2O$	1	50 - 214	$5/2H_2O$	9.45	9.21
	2	214 - 395	$2NH+CO_2$	15.96	15.87
	3	395 - 475	C_8H_4	21.00	20.80
$[Cu(L^3)_2(H_2O)]Cl_2.H_2O$	1	50 - 108	$3H_2O$	4.38	4.08
	2	108 - 172	C_8H_6	8.28	8.22
	3	172 - 228	C_8H_7N	9.51	9.97
$[Ni(L^3)_2].3/2H_2O$	1	50 - 206	$3/2H_2O$	2.39	2.40
	2	205 - 672	$C_{25}H_{12}N_2$	42.47	42.30

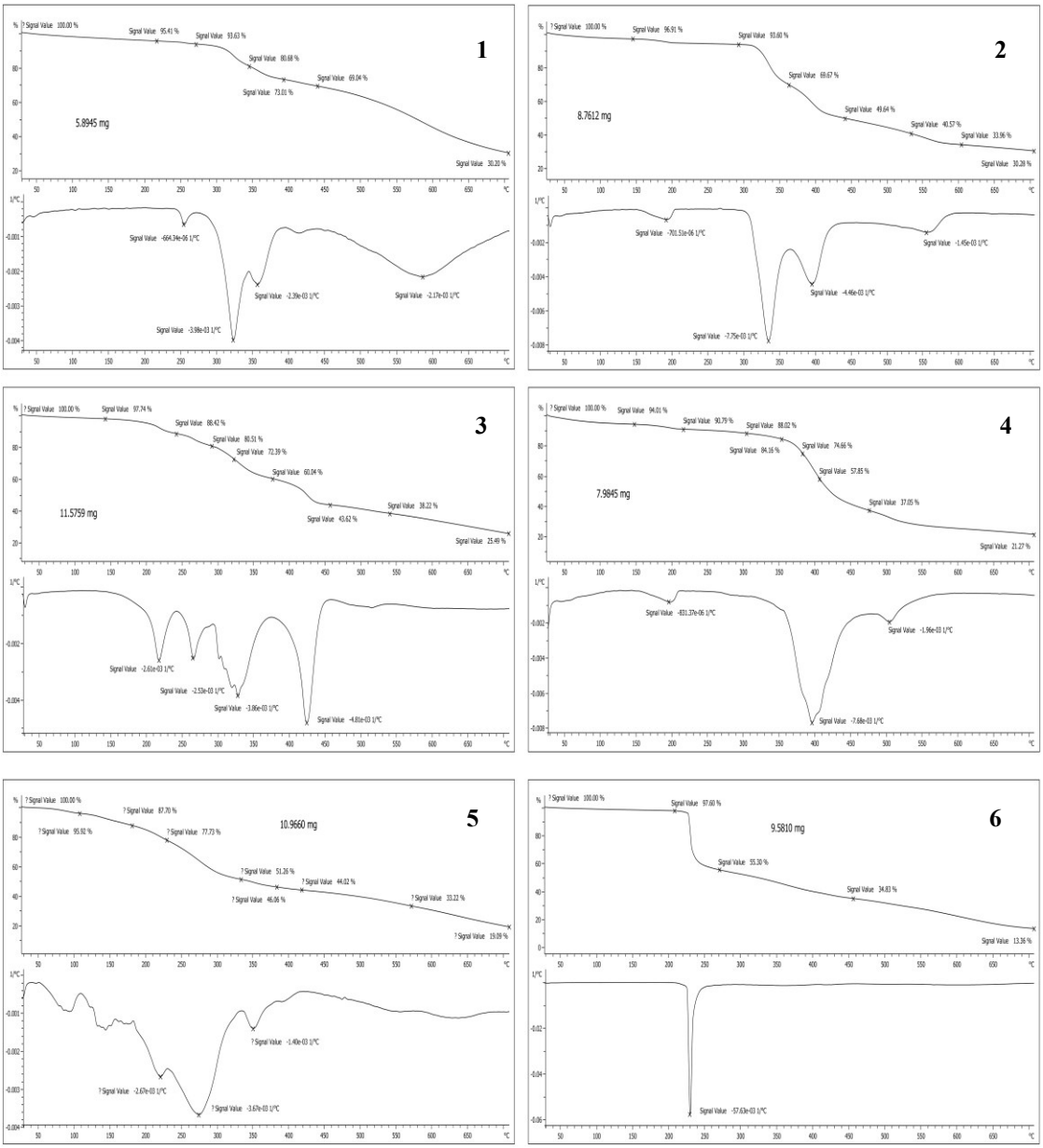

Figure 3 TG Patterns of complexes $[Cu(L^1)(H_2O)_2]Cl_2$(1), $[Ni(L^1)].H_2O$(2), $[Cu(L^2)(H_2O)_2]Cl_2$(3), $[Ni(L^2)].5/2H_2O$(4), $[Cu(L^3)_2(H_2O)_2]Cl_2.H_2O$(5) and $[Ni(L^3)_2].3/2H_2O$(6).

The powder XRD patterns of complexes, **Figure 4** recorded at the range 2θ = 10 – 90 °. Copper complexes, 1 and 3 have crystalline shapes, each showed 4 crystalline peaks at 2θ = 10.91 °, 11.73 °, 15.71 ° and 16.49 ° for complex 1, and 2θ = 13.15 °, 17.64 °, 22.75 ° and 26.01 ° for complex 3. Nickel complexes, 2 and 4 showed a semi-crystalline character through low-split peaks at 2θ = 22.17 °, 22.85 and 29.29 ° for complex 2, and 2θ = 10.68 °, 19.63 ° and 21.76 ° for complex 4. While the L^3 ligand complexes (5 and 6) have shown amorphous properties. The crystallite size of complexes was calculated in nanometer units using the Debye-Scherer equation [23], and found that it was equal to 37.89, 54.90, 48.54 and 31.56 nm for the complexes 1, 2, 3 and 4, respectively.

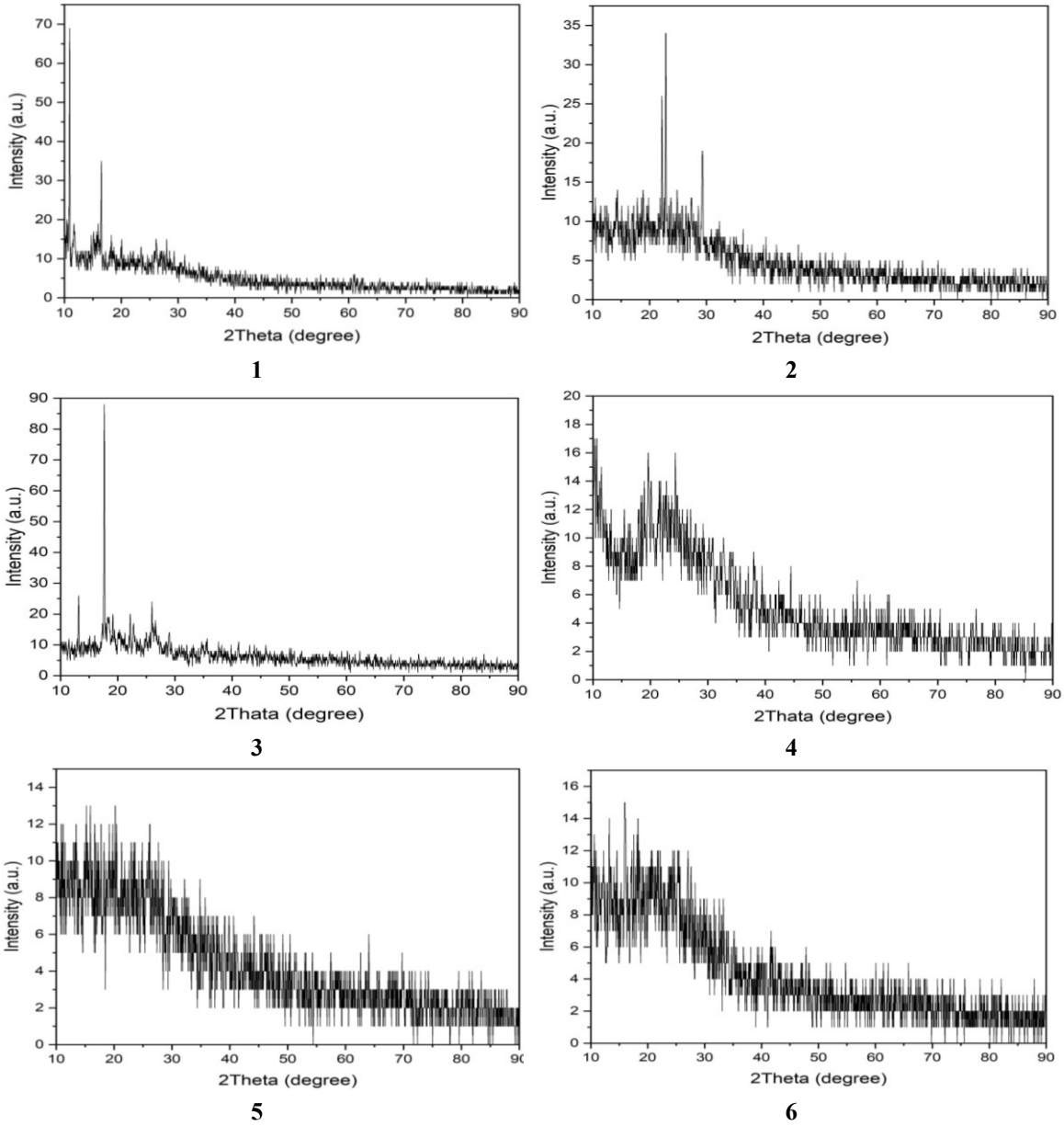

Figure 4 XRD Patterns of complexes $[Cu(L^1)(H_2O)_2]Cl_2$(1), $[Ni(L^1)].H_2O$(2), $[Cu(L^2)(H_2O)_2]Cl_2$(3), $[Ni(L^2)].5/2H_2O$(4), $[Cu(L^3)_2(H_2O)_2]Cl_2.H_2O$(5) and $[Ni(L^3)_2].3/2H_2O$(6).

Anticancer activity

The activity of compounds against breast cancer cells line (MCF-7) was studied using 5 different concentrations (31.25, 62.5, 125, 250, 500 µg/mL) per compounds and the effectiveness of inhibition was calculated at each concentration, in addition to calculating the concentration values of the maximum half effect IC_{50}. All synthesis compounds demonstrated weak anti-cancer activity with IC_{50} values above 70 µg/mL, compared with IC_{50} value of cisplatin as a standard compound (IC_{50}= 1.5 µg/mL) [24]. But 1 compound, complex 5 showed a moderated activity, IC_{50}=8.0 µg/mL with 52.16 % inhibition ratio at the lowest concentration, **Table 2**, which may be due to the presence of chlorine and copper atoms in the structure of complexes.

Table 2 Inhibition ratio of MCF-7 cell line and IC50 values for studied compounds.

Compounds	Conc.(µg/mL)					IC_{50} (µg /mL)
	31.25	62.5	125	250	500	
	Cells inhibition (%)					
L^1	4.73	24.72	32.29	32.46	33.91	1612.3
L^2	22.14	35.52	55.02	58.09	73.89	132.4
L^3	17.79	31.00	43.26	75.34	75.82	132.5
$[Cu(L^1)(H_2O)_2]Cl_2$	25.69	39.87	51.48	56.64	76.30	125.1
$[Ni(L^1)].H_2O$	17.14	51.80	56.64	63.89	65.18	117.6
$[Cu(L^2)(H_2O)_2]Cl_2$	17.31	32.69	42.55	54.09	55.76	76.3
$[Ni(L^2)].5/2H_2O$	25.96	39.01	54.48	56.64	75.30	125.4
$[Cu(L^3)_2(H_2O)]Cl_2.H_2O$	52.16	63.22	63.94	71.87	72.32	8.0
$[Ni(L^3)_2].3/2H_2O$	1.67	9.24	21.01	31.33	64.21	423.7

Molecular docking study

The study of the molecular docking of compound 5 was conducted against breast cancer proteins, MCF-7 cell line which are: ERα (PDP: 3ERT), PR (PDP: 4OAR), EGFR (PDP: 2J6M), mTOR (PDP: 4DRH), CDK2 (PDP: 4FX3), CDK6 (PDP: 3NUP) and Akt (PDP: 5KCV) [25-27]. It was the strongest interaction with 3ERT, 3NUP and 2J6M proteins where it gave the highest affinity energy (S) and the lowest RMSD values [28], **Table 3**. Docking analysis is used to determine how amino acid residues and hydrogen bonds of target proteins interact with compound 5. 2D and 3D forms (**Figure 4**) show a 1 *pi*-interaction of the hydrophobic phenyl moiety with the amino acid Cys-530 of protein 3ERT and 2 hydrogen bonds with 3NUP protein, the first with Lys-129 at a distance of 2.43 Å and other with Asp-102 at a distance of 2.6 Å. While the interaction with protein 2J6M was by forming a hydrogen bond with amino acid Lys-875 with a distance of 2.56 Å, in addition to forming a *pi*-interaction of phenyl ring with amino acid phe-723.

Table 3 Molecular docking data of compound 5 with target 3ERT, 3NUP and 2J6M proteins.

Proteins (Receptors)	RMSD	Affinity energy (S) Kcal/mol	Interaction		
			Type	Amino acid	H-Bonding distance(Å)
3ERT	1.727	−7.432	*pi*-interaction	Cys530	-
3NUP	1.638	−7.360	H-Bonding	Lys129	2.43
			H-Bonding	Asp102	2.67
2J6M	1.9001	−7.351	H-Bonding	Lys875	2.56
			pi-interaction	Phe723	-

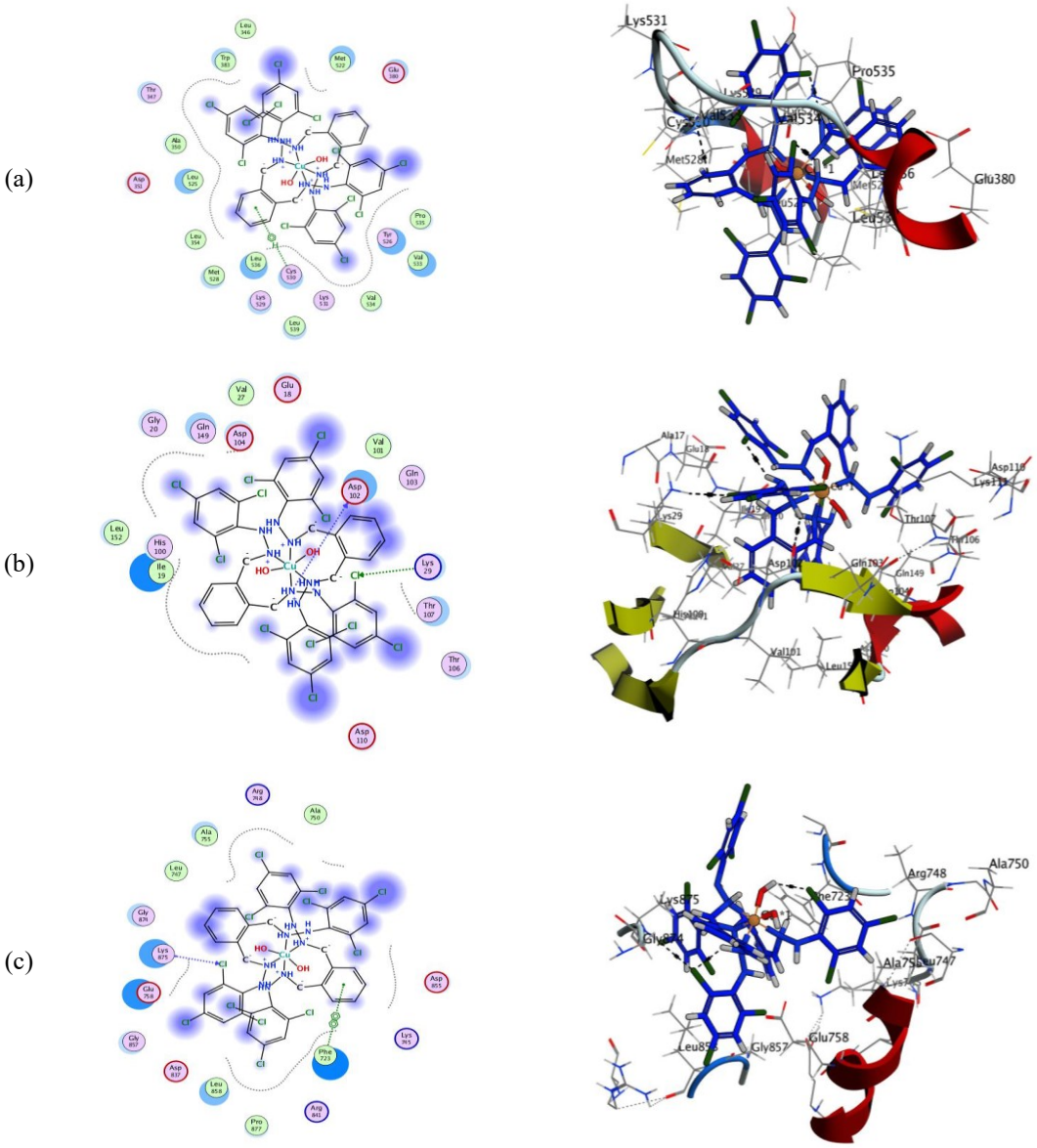

Figure 4 2D and 3D forms of compound 5 with target proteins; (a): 3ERT, (b): 3NUP and (c): 2J6M.

Conclusions

Characterization techniques have validated the proposed structure of the synthesized compounds. L^1 and L^2 acted with Cu^{2+} and Ni^{2+} as a tetra dentate ligands type N_2O_2, while the L^3 was a bi-dentate ligand type N_2. In addition, the geometry of complexes was octahedral (sp^3d^2) with Cu^{2+} and tetrahedral (sp^3) and square planar (dsp^2) with Ni^{2+}. L^1 and L^2 complexes with copper had crystalline properties and with nickel were semi-crystalline, while the L^3 complexes have amorphous characters. The biological study proved that copper complex with L^3 is the only one that is effective against breast cancer (MFC-3 cell line) and it targets ERα, CDK6 and EGFR proteins.

Acknowledgements

The authors extend their thanks and gratitude to the Department of Chemistry, Faculty of Education for Pure Sciences, University of Basra for providing all the facilities related to research, including laboratories, infrared measurements and some other measurements.

References

[1] FM Ahmed, SA Sadeek and WH El-Shwiniy. Synthesis, spectroscopic studies, and biological activity of some new N_2O_2 tetradentate schiff base metal complexes. *Russ. J. Gen. Chem.* 2019; **89**, 1847-83.

[2] AM Abu-Dief and IMA Mohamed. A review on versatile applications of transition metal complexes incorporating schiff bases. *Beni Suef Univ. J. Basic Appl. Sci.* 2015; **4**, 119-33.

[3] RH Al-Asadi, MK Mohammed and HK Dhaef. Mercuration and telluration of 2-fluoro-5-nitroaniline: Synthesis, antibacterial, and computational study. *Russ. J. Gen. Chem.* 2020; **90**, 703-9.

[4] WH El-Shwiniy, LM Abbass, SA Sadeek and WA Zordok. Synthesis, structure, and biological activity of some transition metal complexes with the mixed ligand of metformin and 1,4-diacetylbenzene. *Russ. J. Gen. Chem.* 2021; **91**, 1774-82.

[5] RH Al-Asadi, TA Fahad, BA Saeed and WA Al-Masoudi. Synthesis, characterization and antitumor activity of some new oganotellurium compounds containing azo group, part II. *J. Adv. Chem*. 2014; **8**, 1464-71.

[6] A Arunadevi and N Raman. Biological response of schiff base metal complexes incorporating amino acids - a short review. *J. Coordination Chem.* 2020; **73**, 2095-116.

[7] RH Al-Asadi Synthesis, DFT Calculation and Biological Activity of Some Organotellurium Compounds Containing Azomethine Group. *Orbital Electron. J. Chem.* 2019; **11**, 402-10.

[8] RG Deghadi, AE Elsharkawy, AM Ashmawy and GG Mohamed. Can one novel series of transition metal complexes of oxy-dianiline schiff base afford advances in both biological inorganic chemistry and materials science? *Comm. Inorgan. Chem.* 2022; **42**, 1-46.

[9] P Deveci, B Taner, E Özcan, Z Kılıç, M Karakaya and A Karakas. Structural characterization and second-order nonlinear optical behavior of metal complexes of ferrocene derivative. *Russian J. Gen. Chem.* 2019; **89**, 330-8.

[10] HA Abdullmajed, HA Sultan, RH Al-Asadi, QM Hassan, AA Ali and CA Emshary. Synthesis, DFT calculations and optical nonlinear properties of two derived Schiff base compounds from ethyl-4-amino benzoate. *Phys. Scripta* 2022; **97**, 025809.

[11] BM Ahmed, NA Rudell, I Soto and G Mezei. Reaction of amines with aldehydes and ketones revisited: Access to a class of non-scorpion ate tris(pyrazolyl)methane and related ligands. *J. Org. Chem.* 2017; **82**, 10549-62.

[12] OE Sherif and NS Abdel-Kader. DFT calculations, spectroscopic studies, thermal analysis and biological activity of supramolecular schiff base complexes. *Arab. J. Chem.* 2018; **11**, 700-13.

[13] AA Jambol, MSA Hamid, AH Mirza, MS Islam and MR Karim. Some novel schiff bases from pyruvic acid with amines containing N & S donor atoms: Synthesis, spectral studies and x-ray crystal structures. *Int. J. Org. Chem.* 2017; **7**, 42-56.

[14] T Sujeshwari, E Akila and P Maheswaran. DNA cleavage, antioxidant and antibacterial activity studies of new Schiff base Co(II), Ni(II), Cu(II) and Mn(II) complexes derived from o-phthalaldehyde. *Eur. J. Mol. Clin. Med.* 2020; **7**, 3335-47.

[15] H Köksal, M Dolaz, M Tümer and S Serin. Copper (II), cobalt (III), nickel (II), palladium (II), and zinc (II) complexes of the schiff base ligands derived from 2, 6-diacetylpyridine and phthaldialdehyde. *Synth. Reactivity Inorg. Met. Org. Chem.* 2001; **31**, 1141-62.

[16] Manju, D Kishore and D Kumar. Cadmium and tin complexes of schiff-base ligands. *J. Coordination Chem.* 2011; **64**, 2130-56.

[17] RK Mohapatra, PK Das, MK Pradhan, AA Maihub and MM El-ajaily. Biological aspects of schiff base-metal complexes derived from benzaldehydes: An overview. *J. Iran. Chem. Soc.* 2018; **15**, 2193-227.

[18] N Harbeck, F Penault-Llorca, J Cortes, M Gnant, N Houssami, P Poortmans, K Ruddy, J Tsang and F Cardoso. Breast cancer. *Nat. Rev. Dis. Primers* 2019; **5**, 66.

[19] RH Al-Asadi, WA Al-Masoudi and KSA Al-Rassol. Synthesis, biological activity and computational study of some new unsymmetrical organotellurium compounds derived from (2-amino-5-carboxyphenyl) mercury(II) chloride. *Asian J. Chem.* 2016; **28**, 1171-6.

[20] SA Attique, M Hassan, M Usman, RA Muhammad, S Mahboob, KA Al-Ghanim, M Bilal and MZ Nawaz. A molecular docking approach to evaluate the pharmacological properties of natural and synthetic treatment candidates for use against hypertension. *Int. J. Environ. Res. Public Health* 2019; **16**, 923.

[21] FA Nawar, RH AL-Asadi and DS Abid. Synthesis, antibacterial activity and DFT calculations of some Thiazolidine-4-Carboxylic acid derivatives and their complexes with Cu(II), Fe(II) and VO(II). *Egyptian J. Chem.* 2020; **63**, 349-62.

[22] L Mitu, M Ilis, N Raman, M Imran and S Ravichandran. Transition metal complexes of Isonicotinoyl-hydrazone-4-diphenylaminobenzaldehyde: Synthesis, characterization and antimicrobial studies. *J. Chem.* 2012; **9**, 298175.

[23] S Velumani, X Mathew and PJ Sebastian. Structural and optical characterization of hot wall deposited $CdSe_xTe_{1-x}$ films. *Sol. Energ. Mater. Sol. Cells* 2003; **76**, 359-68.

[24] S Fani, B Kamalidehghan, KM Lo, NM Hashim, KM Chow and F Ahmadipour. Synthesis, structural characterization, and anticancer activity of a monobenzyltin compound against MCF-7 breast cancer cells. *Drug Des. Dev. Ther.* 2015; **23**, 6191-201.

[25] DH Fagan, LM Fettig, S Avdulov, H Beckwith, MS Peterson, YY Ho, F Wang, VA Polunovsky and D Yee. Acquired tamoxifen resistance in MCF-7 breast cancer cells requires hyperactivation of eIF4F-mediated translation. *Hormones cancer* 2017; **8**, 219-29.

[26] K Venugopal, H Ahmad, E Manikandan, KA Thanigai, K Kavitha, M Moodley, K Rajagopal, KR Balabhaskar and M Bhaskar. The impact of anticancer activity upon *Beta vulgaris* extract mediated biosynthesized silver nanoparticles (ag-NPs) against human breast (MCF-7), lung (A549) and pharynx (Hep-2) cancer cell lines. *J. Photochemistry Photobiology B Biol.* 2017; **173**, 99-107.

[27] C Dong, J Wu, Y Chen, J Nie and C Chen. Activation of PI3K/AKT/mTOR pathway causes drug resistance in breast cancer. *Front. Pharmacol.* 2021; **12**, 628690.

[28] DZ Mutlaq, AA Al-Shawi and RH Al-Asadi. Synthesis, characterization, anticancer activity, and molecular docking of novel maleimide-succinimide derivatives. *Egyptian Pharmaceut. J.* 2021; **20**, 303-12.